Nonradiative recombination via strongly localized defects in quantum wells

P. Michler, T. Forner, V. Hofsäß, F. Prins, K. Zieger, F. Scholz, and A. Hangleiter
4. Physikalisches Institut, Universität Stuttgart, Pfaffenwaldring 57, D-70550 Stuttgart, Germany
(Received 17 December 1993)

Using time-resolved photoluminescence, we have studied the nonradiative recombination of excess charge carriers in oxygen-implanted $GaAs/Al_{0.4}Ga_{0.6}As$ single quantum wells. In order to reveal the recombination mechanism, the carrier lifetime is measured as a function of temperature and well width. We observe a decrease of the measured lifetime with increasing implantation dose and the nonradiative part of the recombination rate increases with increasing temperature. We find that the nonradiative recombination is thermally activated and the activation energies increase with decreasing well width. Under the assumption of strongly localized deep impurities we can explain this behavior with multiphonon capture processes and an analysis of the well-width dependence of the activation energies allows for the determination of the coupling strength for electron capture. In agreement with deep-level transient-spectroscopy (DLTS) measurements we determine a deep level 430 meV below the conduction band.

The recombination of excess carriers in quantum wells (QW's) has been an extensively studied subject for many years. Previous theoretical and experimental work on radiative recombination provided a good understanding of the radiative exciton lifetime[1,2] in QW's and of the temperature-dependent effects of exciton ionization on carrier lifetime.[3–5] Recent time-resolved and continuous-wave photoluminescence (PL) studies have revealed the importance of thermal emission of carriers into the barriers at higher temperatures.[6–8] The thermal escape into the barriers is a nonradiative loss mechanism for the carriers in the wells which leads to a strong reduction of the PL intensity and PL lifetime in the QW. The efficiency of this process depends on the effective confinement energy of the carriers in the QW and is therefore large in QW's with low barriers (e.g., $GaAs/Al_xGa_{1-x}As$ or $GaInP/Al_xGa_{1-x}InP$ with low Al content) and in thin QW's, with only a few monolayer thickness, respectively. In QW's with high effective-confinement energies, processes like interface recombination or nonradiative recombination via deep impurity levels can become important. The basic understanding of such processes is of fundamental interest and of considerable relevance for many applications.

Nonradiative recombination via deep impurity levels is normally described in terms of the Shockley-Read-Hall model,[9,10] where electrons and holes can recombine by successive capture into the deep impurity level. During these two transitions, an energy equal to the energy gap must be dissipated and the basic question is about the mechanism of the energy loss. Up to now, most of the investigations concerning the energy loss mechanism were carried out in bulk material, particularly in GaAs, with capacitance transient methods[11] and time-resolved PL.[12] Many of the results are consistent with multiphonon capture processes. To our knowledge, comparable investigations with regard to the energy loss mechanism in QW's have not been reported up to now. On one hand it is important to clarify the question of the physical mechanism of carrier capture into deep impurity levels in the QW's. On the other hand, the degree of localization of the potential of such deep centers must be considered in a theory dealing with nonradiative capture. The degree of localization is determined through the ratio between the extension of the potential of the deep impurity and the QW width. In the case of weak localization, i.e., the extension of the potential of the deep impurity is comparable to or larger than the QW width, the energy levels of the deep impurity are quantized, whereas in the case of strong localization the energetic difference to the three-dimensional conduction and valence bands is unchanged. As a consequence, in the strong localization limit, the energetic distance between the deep-level energy and the electron and hole subbands becomes a function of the well width since the quantization of the subbands depends on well width.

In this paper we present a systematic study of the nonradiative recombination in oxygen-implanted $GaAs/Al_{0.4}Ga_{0.6}As$ QW's as a function of temperature and well width. It includes a model which shows that the temperature dependence of the electron capture coefficient is consistent with a multiphonon process and allows for the determination of the coupling strength for electron capture and of the energetic depth of the deep level.

As starting material we used $GaAs/Al_{0.4}Ga_{0.6}As$ single quantum wells (SQW's) grown by metal-organic vapor phase epitaxy (MOVPE) on a GaAs substrate kept at a temperature of about 700 °C. The investigated well widths L_z are 3, 5, 8, 10, and 50 nm. The SQW's are sandwiched between $Al_{0.4}Ga_{0.6}As$ barriers, where the barrier width on the surface side is 100 nm and the barrier width on the substrate side is 1.5 μm thick. Owing to the spillover of carriers from the barriers to the wells, the majority carrier concentration of unintentionally doped QW's depends on the background dopant level of the barriers.[13] Since the background dopant is p type in our MOVPE-grown $Al_{0.4}Ga_{0.6}As$ material, we

conclude that the holes are the majority carriers in the QW's. The absolute value of the radiative lifetime at a certain temperature is governed by the majority carrier concentration.[13] If we compare the absolute value of the radiative lifetime from the 5 nm QW [τ_r(300 K) = 4 ns] with recently published calculated values from Ridley,[3] we can deduce a majority carrier concentration of about $p^{\mathrm{maj}} \approx 3.2 \times 10^{11}$ cm^{-2} in the wells. This has the important consequence that we can neglect excitonic effects, since in this carrier density region strong exciton screening takes place and almost only free carriers are present.[3,5] We find in all unimplanted samples an increase of the experimentally observed lifetime with increasing temperature, in good agreement with the temperature dependence of radiative recombination in a quantum well.[5] This means that the determined slopes $\gamma \approx (1.1\text{–}1.3)$ are in good agreement with theory where it is expected that $\tau_r \sim T^{\gamma}$ with $1 \leq \gamma \leq 1.5$ for such high carrier densities.[5,13] High Al content ($x_{\mathrm{Al}} = 0.4$) was used in the barrier because of the large band offset with respect to GaAs. As a consequence, thermal emission processes can be neglected in our samples up to temperatures of 200 K even for the QW with the smallest well width of $L_z = 3$ nm. The deep levels were introduced by oxygen implantation. The choice of this method was influenced by its technological importance on one hand and by the possibility to control the impurity concentration reproducibly over a wide range of doses on the other hand. We choose an implantation energy of 75 keV. As a consequence the theoretical maximum of the Gaussian distribution[14] of the implanted oxygen ions is centered in the middle of the QW. The full width at half maximum (FWHM) of the oxygen distribution is 45 nm which means that one can assume a homogeneous distribution of radiation defects in the QW's with L_z in the range 3–10 nm. This would not hold true for the sample with $L_z = 50$ nm. Therefore we have made two implantations with energies of 55 and 85 keV which lead to a slightly varying defect profile with the same averaged bulk concentration of defects in the sample. The samples were implanted with dose rates ranging from 2.3×10^{12} to 2.3×10^{13} cm^{-2}, which correspond to oxygen densities between 2×10^{17} and 2×10^{18} cm^{-3} in the QW's. After implantation the samples were annealed for 1 min at a temperature of 875 °C with a rapid thermal annealing process.

The time-resolved measurements were performed using a photoluminescence setup, where the samples were excited by 5 ps pulses from a synchronously pumped mode-locked cavity-dumped dye laser. We used R6G, which made it possible to tune the excitation energy below the gap of the $Al_{0.4}Ga_{0.6}As$ barrier, to generate the excess carriers only in the GaAs wells. The carrier density was estimated from the excitation power density and the absorption coefficient of GaAs to be about $(2\text{–}5)\times 10^{10}$ cm^{-2} in the wells. The luminescence was detected with a microchannel plate photomultiplier (with S 25 response). The PL decays were measured with a time-correlated photon-counting technique. The time resolution of the system is about 150 ps.

Typical decay curves from the time-resolved PL measurements are shown in Fig. 1 before and after oxygen implantation with three different doses for a 5 nm well. Each PL decay was measured at the peak of the emission line. We find that the experimental data are consistent with a pure exponential decay with time constant τ_{PL} over at least one and a half orders of magnitude. We observe a decrease of the decay time τ_{PL} with increasing dose. This shows clearly that the number of nonradiative defects increases with increasing implantation dose.

In order to evaluate the dominant recombination mechanism we have done systematic temperature-dependent lifetime measurements, which are summarized in Fig. 2 for a 3 nm QW before and after implantation. For the reference sample we find an increase of the experimentally observed lifetime with increasing temperature, which is in good agreement with the temperature dependence of radiative recombination in a two-dimensional semiconductor.[5] Obviously the time constants of the oxygen-implanted QW's decrease systematically with increasing implantation dose and the difference between the time constants of the reference sample and the implanted samples increases with increasing temperature. This means that the nonradiative fraction of the total recombination increases toward higher temperature. The measured decay time τ_{PL} at temperature T is connected to the radiative and nonradiative recombination times τ_R and τ_{NR}, respectively, by

$$\frac{1}{\tau_{\mathrm{PL}}} = \frac{1}{\tau_R} + \frac{1}{\tau_{\mathrm{NR}}} , \tag{1}$$

where the radiative decay time τ_R can be expressed as $\tau_R^{-1} = Bp^{\mathrm{maj}}$. Here B is the radiative rate constant and p^{maj} is the concentration of the majority carriers. Under the assumption that the majority carrier concentration in the samples is unchanged after oxygen implantation, which was confirmed by deep-level transient-spectroscopy (DLTS) measurements in our oxygen-implanted bulk

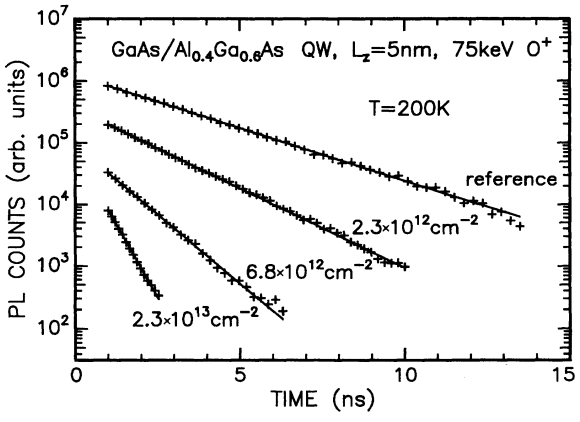

FIG. 1. Typical decay curves from 5 nm single quantum wells after oxygen implantation with different implantation doses. Also shown is the PL decay of the untreated reference sample. The solid curves give the fit to experimental points assuming a monoexponential decay. The curves are vertically shifted and shown on a logarithmic scale.

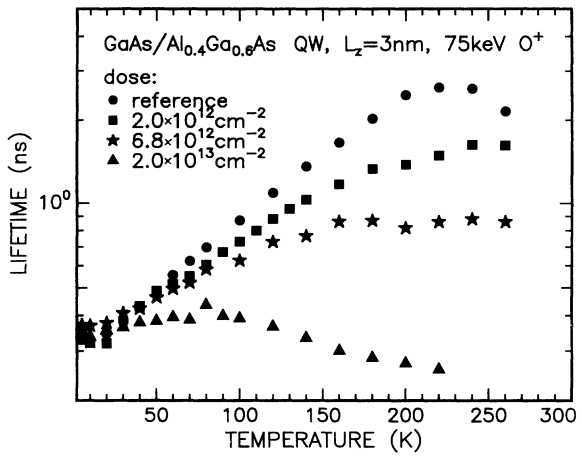

FIG. 2. Temperature dependence of the PL decay time τ_{PL} from 3 nm single quantum wells for different implantation doses. Also shown is the temperature dependence of the PL decay time of the untreated reference sample.

samples, the nonradiative lifetime τ_{NR} can be extracted with the measurements of τ_R (before implantation) and τ_{PL} (after implantation).

The temperature dependence of the nonradiative lifetime τ_{NR}, reported in Fig. 3, is similar for all the QW's investigated. We find for all oxygen-implanted QW's a thermally activated decrease of the nonradiative lifetime with an activation energy depending on well width. The activation energies (see Fig. 3) obtained from the slopes of the measured nonradiative lifetimes increase with decreasing thickness of the QW. This can be explained with a model for the carrier capture which takes into account the well-width dependence of the quantization energy on one hand and the strong localization of the deep-level

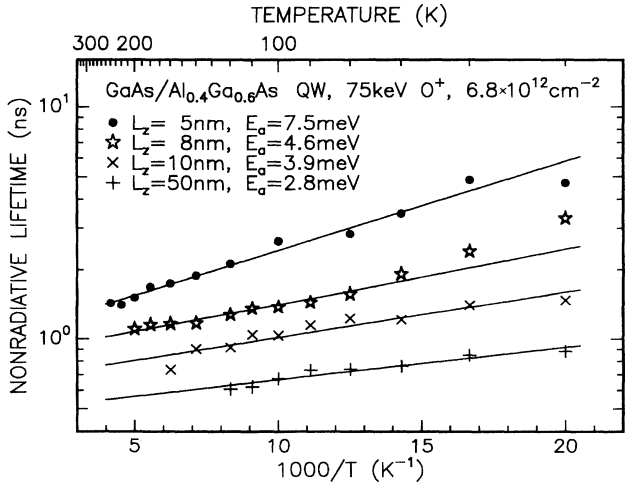

FIG. 3. Temperature dependence of the nonradiative lifetime τ_{NR} for different well thicknesses. The straight lines are the best fits to the experimental data assuming a thermally activated behavior and correspond to values E_a = 2.8, 3.9, 4.6, and 7.5 meV.

center on the other hand. This will be discussed in more detail below.

Furthermore, it is striking that the absolute values of the nonradiative lifetime decrease with increasing well width. This trend can be understood under the assumption that the two-dimensional density of deep centers N^0_{2D} is the relevant quantity for nonradiative recombination in QW's. A constant three-dimensional density of deep centers was produced through the oxygen implantation. As a consequence, the two-dimensional density of deep centers increases with increasing well width according to $N^0_{2D} = N^0_{3D} L_z$, which leads to a decrease of the nonradiative lifetime with increasing well width.

In order to discuss the nonradiative capture mechanism one has to extract the capture coefficents from the nonradative lifetimes τ_{NR}. Since the background doping is p type in the $Al_xGa_{1-x}As$ barriers, the electrons are the minority carriers in the QW's. As a consequence the nonradiative low-injection lifetime of a single-level donor-like deep impurity is given by[15]

$$\tau_{NR}(T) = \frac{1}{C_n(T) N^0(T)} , \tag{2}$$

where $C_n(T)$ is the electron capture coefficient and $N^0(T)$ is the density of neutral recombination centers. If the equilibrium Fermi level is not located near the impurity energy level, the concentration of neutral impurity states N^0 will not depend on temperature.[16] The Fermi level E_F in the $Al_{0.4}Ga_{0.6}As$ barrier is located near the valence band ($E_F - E_V < 150$ meV) for the whole temperature range (5 K $< T <$ 220 K) examined. DLTS measurements for oxygen-implanted bulk GaAs samples yield a trap level 430 $\pm$ 10 meV below the conduction band, far away from the equilibrium Fermi level in the p-type QW's. Furthermore, we observe no change in the injection dependence of the lifetime which is expected if thermal ionization of the deep level takes place.[16] Therefore the measured temperature dependence of the nonradiative lifetime gives us the real temperature dependence of the electron capture coefficients. Consequently, the electron capture coefficients derived from these data are thermally activated.

From the increase of the capture coefficients with temperature, multiphonon capture[17] seems to be the most reasonable model from the theoretical point of view. The multiphonon theory predicts a thermally activated behavior of the capture coefficients at high temperatures,[18] in coincidence with our experimental findings. Classically, the activation energy is necessary to overcome an energy barrier during the transition from a band (conduction or valence band) to the highly excited deep-level state. The height of the energy barrier for such a transition depends on the energetic difference between the corresponding band and the deep-level state on one hand and on the Huang-Rhys factor[19] S on the other hand. The Huang-Rhys factor S characterizes the strength of the electron-phonon interaction. Therefore one activation energy is characteristic for one sort of deep level in bulk samples.

In contrast, in the case of strong localization, the en-

ergetic distance between the first subband and the deep-level state in a QW is a function of well width. In this case the energetic level of the deep center is independent of well width whereas the electron and hole subbands depend on well width since the quantization of the subbands depends on well width. This means that one expects for one sort of deep center in QW's different activation energies, depending on well width. This is visualized in the configuration coordinate (CC) diagram in Fig. 4 for the case of electron capture. In the CC diagram the sum of electronic and lattice potential energy is shown versus a single normal coordinate q known as the configuration coordinate. The two upper parabolas (E_{L1}, E_{L2}) represent the lowest subbands of two QW's with different thicknesses ($L_{z1} < L_{z2}$). The parabola E_{L1} of the QW with smaller well width lies above the parabola of the QW with the larger well width because of the larger quantization energy. The lowest parabola represents the deep-level center. In terms of this CC sheme, a nonradiative capture transition therefore can take place only at the crossing points of the parabolas. Generally a characteristic thermal energy E_{a1}, E_{a2} is necessary to reach the crossing points and it is obvious from Fig. 4 that the activation energy E_a increases with decreasing well width. This behavior was observed in the oxygen-implanted QW's and the multiphonon model is adequate to explain qualitatively the observed temperature and well-width dependence of the capture coefficients.

It is very interesting to analyze the well-width dependence of the activation energies coming from the slopes from Fig. 3 in somewhat more detail. If the electron-lattice interaction is linear in the lattice coordinate q and the vibrations are harmonic, the potential curves in Fig. 4 will be parabolas with identical frequencies but different equilibrium positions for the deep level and the subbands.[20] Then it follows from Fig. 4 that at crossover

$$E_{ai} = \frac{(E_0 + E_{Qi} - S\hbar\Omega)^2}{4S\hbar\Omega} , \tag{3}$$

where S is the Huang-Rhys factor and $\hbar\Omega$ is the phonon energy of the emitted phonons. The experimentally determined activation energies are shown in Fig. 5 as a function of the quantization energies.

It is important to note here that the annealing process around 875 °C produces Al interdiffusion across the heterointerfaces. The extend of the interdiffusion process is characterized by a diffusion length L_d. One can calculate the Al diffusion length L_d from the observed emission energy shift between the implanted and the corresponding unimplanted QW's.[21] We have determined the diffusion length in our samples (dose = 6.8×10^{12} cm^{-2}) to be $L_d = 0.3$ nm. The modification of the Al profile leads to change in the shape of the confinement potentials for electrons and holes. The quantization energies for the implanted samples are calculated numerically taking an error function for the confinement potentials for the slightly interdiffused QW's.[21]

Using the expression for the quantization energy dependence of the activation energy from Eq. (3) we have analyzed the data of Fig. 5 and determined an energy level of 461 ± 40 meV below the conduction band, and a Huang-Rhys factor S of 12.6 ± 2 taking a phonon energy $\hbar\Omega$ of 36 meV. The comparable value of the product $S \times \hbar\Omega = 454$ meV with the energetic depth of the deep level $E_L - E_T = 461$ meV indicates a middle-strength coupling between the electronic level and the lattice. We

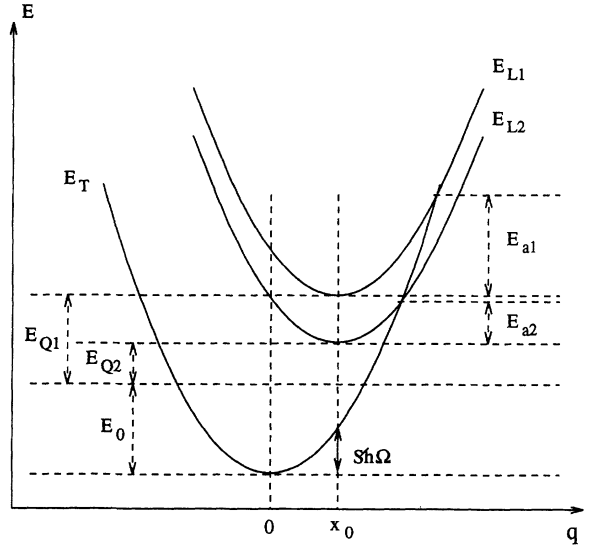

FIG. 4. Configuration coordinate diagram showing the effective lattice potential curves as a function of the associated configurational coordinate q, assuming a linear electron-lattice interaction and a harmonic potential. Symbols: E_{L1}, E_{L2}, lowest electron subbands of two QW's with different well thickness ($L_{z1} < L_{z2}$); E_T, energy position of the deep level; E_{Q1},E_{Q2}, quantization energies of QW1 and QW2; E_{a1},E_{a2}, activation energies of QW1 and QW2; E_0 energetic depth of the deep level in bulk material; S, Huang-Rhys factor; and $\hbar\Omega$, effective phonon energy.

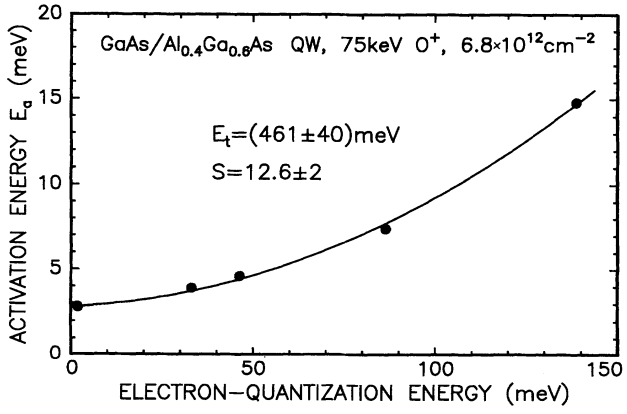

FIG. 5. Quantization energy dependence of the measured thermal activation energies. The solid line is the best fit to the data using Eq. (3) and yields the Huang-Rhys factor S and the energetic difference E_T between the conduction band and the deep level.

find a good agreement between the value of the deep level coming out of this analysis with the result from the DLTS measurements $E_L - E_T = 430 \pm 10$ meV. This supports the assumption that this deep level is responsible for the nonradiative recombination process in the oxygen-implanted QW's. This deep level was also found in high energy (2 MeV) proton and low energy (60 keV) Ar ion irradiated bulk GaAs samples.[22] Therefore it seems reasonable that this deep center is damage induced and not specially oxygen correlated.

In summary, we have presented an experimental study of nonradiative recombination via a deep impurity level in oxygen-implanted GaAs/$Al_{0.4}Ga_{0.6}As$ SQW's. Our experiments show thermally acitivated nonradiative recombination processes with increasing activation energies for decreasing well widths. This can be explained by multiphonon capture processes with the requirement of strongly localized deep impurities, i.e., the extension of the potential of the deep impurity level is small with respect to the width of the QW. We find a Huang-Rhys factor of 12.6 for the electron capture and a deep level to 461 meV below the conduction band, in good agreement with the DLTS result $E_L - E_T = 430 \pm 10$ meV.

We would like to thank W. Kürner for the DLTS measurements. The financial support of this work by the Deutsche Forschungsgemeinschaft under Contract No. Ha 1670/1 is gratefully acknowledged.

[1] J. Feldmann, G. Peter, and E. O. Göbel, Phys. Rev. Lett. **59**, 2337 (1987).
[2] D. S. Citrin, Phys. Rev. B **47**, 3832 (1993).
[3] B. K. Ridley, Phys. Rev. B **41**, 12 190 (1990).
[4] P. Michler, A. Hangleiter, A. Moritz, V. Härle, and F. Scholz, Phys. Rev. B **47**, 1671 (1993).
[5] A. Hangleiter, Phys. Rev. B **48**, 9146 (1993).
[6] G. Bacher, H. Schweizer, J. Kovac, and A. Forchel, Phys. Rev. B **43**, 9312 (1991).
[7] P. Michler, A. Hangleiter, M. Moser, M. Geiger, and F. Scholz, Phys. Rev. B **46**, 7280 (1992).
[8] S. Marcinkevičius and U. Olin, J. Appl. Phys. **74**, 3587 (1993).
[9] W. Shockley and W. T. Read, Phys. Rev. **87**, 835 (1952).
[10] R. N. Hall, Phys. Rev. **87**, 387 (1952).
[11] C. H. Henry and D. V. Lang, Phys. Rev. B **15**, 989 (1977).
[12] P. Michler, A. Hangleiter, R. Dieter, and F. Scholz, J. Appl. Phys. **72**, 4449 (1992).
[13] G.W. 't Hooft, M. R. Leys, and H. J. Talen-v.d. Mheen, Superlatt. Microstruct. **1**, 308 (1985).
[14] J. F. Ziegler, *Handbook of Ion Implantation Technology* (North-Holland, Amsterdam, 1992).
[15] G. K. Wertheim, Phys. Rev. **109**, 1086 (1958).
[16] A. Hangleiter, Phys. Rev. B **35**, 9149 (1987).
[17] T. N. Morgan, Phys. Rev. B **28**, 7141 (1983).
[18] R. Pässler, Phys. Status Solidi B **85**, 203 (1978).
[19] K. Huang and R. Rhys, Proc. R. Soc. London Ser. A **204**, 406 (1950).
[20] P. T. Landsberg, *Recombination in Semiconductors* (Cambridge University Press, Cambridge, England, 1991), p. 453.
[21] H. Leier, A. Forchel, G. Hörcher, J. Hommel, S. Bayer, and H. Rothfritz, J. Appl. Phys. **67**, 1805 (1990).
[22] Y. Yuba, M. Matsuo, K. Gamo, and S. Namba, in *Proceedings of the 13th International Conference on Defects in Semiconductors, Coronado, CA, 1984*, edited by L. C. Kimerling and J. M. Parsey, Jr. (Metallurgical Society of AIME, New York, 1985), p. 973.